Desalination and Water Treatment
www.deswater.com

doi:10.5004/dwt.2017.0259

59 (2017) 191–201
January

Use of azomethine-bridged phenolic metallophthalocyanines for sensitization of TiO_2

Melek Koç[a], Cansu Albay[a], İlknur Altın[a], Rıza Bayrak[b], Halil Gökce[c], İsmail Değirmencioğlu[a,*], Münevver Sökmen[a,*]

[a]*Karadeniz Technical University, Faculty of Science, Department of Chemistry, 61080 Trabzon, Turkey, Tel. +90 462 3773321; Fax: +904623253196, email: ismail61@ktu.edu.tr (İ. Değirmencioğlu); Tel. +90 462 3772532; emails: msokmen@ktu.edu.tr (M. Sökmen), melekim_kimyaci@hotmail.com (M. Koç), cansualby_08@hotmail.com (C. Albay)*
[b]*Sinop University, Vocational School of Health Services, Department of Medical Laboratory Techniques, 57000 Sinop, Turkey, email: bayrakriza@sinop.edu.tr*
[c]*Giresun University, Vocational High School of Health Services, Güre Campus, 28200, Giresun, Turkey, email: halilgokce.hg@gmail.com*

Received 7 March 2016; Accepted 22 June 2016

ABSTRACT

A group of novel azomethine-bridged phenolic metallophtalocyanines (substituted at nonperipheral position, MPc) were synthesized, characterized and used as sensitizer. Phthalocyanine derivatives (containing TiO(II), Fe(II), Co(II), Ni(II) and Zn(II) ions in the center of phtalocyanine) were immobilized on TiO_2 photocatalyst using a wet deposition method. MPc/TiO_2 nanocomposites have been tested for their photocatalytic reduction ability of Cr(VI) ions in aqueous solution under near visible light irradiation. The results demonstrated that the presence of the sensitizer is certainly beneficial for the photocatalytic activity of TiO_2, confirming the significant role of substitution and metal co-ordination in the center of the phthalocyanine ring. Photoreduction results show that the all composite materials exposed significantly higher Cr(VI) removal performance than bare TiO_2. Consequently, MPc sensitized TiO_2 nanocomposites may be good alternatives for efficient photocatalysis that can be used for wastewater treatment processes.

Keywords: Dye sensitization; Metallophtalocyanines; Photocatalysis

1. Introduction

Metallophthalocyanines (MPc) are a family of tetrapyrrole derivatives showing interesting properties coupled with high absorption coefficient in the visible region, high stability to chemical, thermal and hard conditions [1]. Synthesis of novel MPc derivatives has recently received great attention in various industrial applications such as catalyst, dye-sensitization, photodynamic cancer therapy, chemical sensors and solar energy conversion [2–7]. Unsubstituted phthalocyanines are known to have low solubility in either aqueous media or inorganic solvents. The solubility of these compounds can be increased by designing the peripheral or nonperipheral substitution on main macrocyclic ring. Substituents containing long alkyl chains with nitrogen or sulfur and large groups are beneficial for both solubility and facilitating electron transfer [8,9]. Some researchers have reported that several ions such as zinc, iron, and copper can be incorporated into phthalocyanine core to obtain new molecules exposing novel properties. Therefore, both specified substitution and corporation metal ions into macrocyclic ring might have a positive effect on electron transfer.

The utilization of TiO_2-heteregeneous photocatalytic process for photo-removal of various pollutants in aqueous media is a hot topic research in economical and environmental friendly processes [10–12]. However, photocatalytic activity of TiO_2 is limited by high recombination rate of electron-hole pairs and low absorption in visible range [13,14]. Dye sensitization is proposed to over-

*Corresponding authors.

1944-3994 / 1944-3986 © 2017 Desalination Publications. All rights reserved.

whelm this defect [15]. Phthalocyanine-TiO_2 hybrid composite extends the light absorption to visible range. There are only a few studies that involves MPc (has polar substituents such as sulfonic acid groups on the macrocyclic ring) as sensitizer in the TiO_2 mediated photocatalytic reactions for removal of organic/inorganic based pollutants from water [16–18]. In a typical phthalocyanine sensitization reaction, MPc absorbs the light to produce excited MPc* immobilized on TiO_2. This excitation generate singlet oxygen ($^1O_2$) by energy transfer, followed by generation of the cation radical (MPc^+) and conduction band electrons (e_{cb}^-) of TiO_2 [19]. Electron injection at TiO_2 surface was faster than electron back-transfer from the conduction band to the MPc radical. Therefore, electron-hole recombination rate can be suppressed. Consequently, the electrons reacted with dissolved oxygen molecules and $^1O_2$ to form hydroxyl radical for the oxidation of organics. At the same time, inorganic pollutants such as Cr(VI) ions are reduced to nontoxic Cr(III) via the excited electrons, which are transferred to conduction band of TiO_2. In a study published by Huang et al. [20], zinc phthalocyanine (ZnPc) was supported on TiO_2-SiO_2 microparticles (ZnPc-SiO_2-TiO_2) by covalent bonds to produce photosensitizer. The photocatalytic efficiency of the prepared ZnPc-SiO_2-TiO_2 was evaluated for the decomposition of methylene blue (10 mg/L) under visible light irradiation. Their results revealed that ZnPc-SiO_2-TiO_2 had great photocatalytic activity than other catalysts. In another study, Zhao et al. [21] report the in situ synthesis of CoPc/TiO_2 nanocomposite through the annulations of 1,2-dicyanobenzene on the surface of TiO_2 with Co(II) as template. Experimental results demonstrated that CoPc/TiO_2 is a highly efficient photocatalyst for CO_2 reduction to formic acid, methanol and formaldehyde.

In this study, we have synthesized a new class of MPc with azomethine-bridged phenolic groups (methylated and ethylated derivatives) substituted at nonperipheral position. The R groups were specifically designed to increase the polarity of MPc (for a better attachment on TiO_2) and facilitate the electron transfer. Azomethine-bridged phenolic substitution meets all necessary requirements for an effective light harvesting. Apart from substitution on Pc ring, the central metal ion may play an important role on electron transfer. The main Pc ring contains five metals ions such as titan oxide, iron, cobalt, nickel and zinc. Ten MPc derivatives are totally new; structural evaluation and spectroscopic characterizations of synthesized phthalocyanines are being first time reported here. The absorption of photons is the first step of TiO_2-heteregeneous photocatalytic process that causes formation of the excited state dye by electron transfer from the ground state. Then the electron is transferred to the conduction band of the semiconductor from the lowest unoccupied molecular orbital (LUMO) of the dye. Because the recombination of the photogenerated excitons is a parasitic reaction that causes to the fluorescence of the dye, this process must be very rapid. Therefore, to better understand the working of the system, the theoretical investigation of the light absorption properties of the azomethine-bridged phenolic dyes is very important, as well as the design of new similar dyes with improved performances. To this end, in the present paper, we reveal a theoretical investigation by Density Functional Theory (DFT) computation of ten substituted Pcs to better understand the reduction capacity of Cr(VI) ion.

This study is mainly concentrated on the synthesis of a group of novel azomethine-bridged phenolic phthalocyanines that have metal ions in the center of macrocyclic ring. Two different substituted groups namely methylated and ethylated nonperiferal MPc derivatives were used as sensitizer dye. The paper comprises largely synthesis of sensitizer molecules, details of synthesis steps and structural confirmation.

MPc/TiO_2 (namely, TiOPc/TiO_2, FePc/TiO_2, CoPc/TiO_2, NiPc/TiO_2 and ZnPc/TiO_2) nanocomposites were prepared using wet deposition method. Photocatalytic activity of the prepared composites was investigated by measuring the reduction of Cr(VI) ions as a test pollutant. Cr(VI) ions have been chosen as a model heavy metal pollutant owing to its toxicity and carcinogenic properties [22].

2. Materials and methods

2.1. Materials

All reagents were analytical grade and used without further purification. TiO_2 nanopowder (anatase) was purchased from Sigma-Aldrich (Darmstadt, Germany) with average particle size about 44 nm. Reactions were carried out under dry and oxygen-free nitrogen atmosphere using standard Schlenk techniques. 1,8-diazabicyclo[5.4.0]undec-7-ene (DBU) was purchased from Fluka Riedel-de Haen. Initially, (E)-3-(4-(4-(dimethylamino)benzylideneamino)phenoxy)-phthalonitrile (1) and (E)-3-(4-(4-(diethylamino)benzylideneamino)phenoxy)-phthalonitrile (2) were synthesized following the procedure given in our previous work [İ. Değirmencioğlu, unpublished data]. All solvents were dried and purified as described by Perrin and Armarego before use [23].

2.2. Equipments

^{1}H-NMR spectra were recorded on a Varian XL-200 NMR spectrophotometer in deuterated chloroform ($CDCl_3$) and dimethyl sulfoxide-d_6 (DMSO-d_6), and chemical shifts were reported (δ) relative to Me_4Si as internal standard. Fourier transform infrared spectroscopy (FT-IR) spectra were recorded on a PerkinElmer Spectrum one FT-IR spectrometer. The mass spectra were measured with a Micromass Quattro LC/ULTIMA LC-MS/MS spectrometer using chloroform–methanol as solvent system. All experiments were performed in the positive ion mode. Melting points were measured on an electrothermal apparatus and are uncorrected. Absorption spectra in the UV-visible region were recorded with a Shimadzu 2101 UV-Vis spectrophotometer. Photocatalytic experiments are carried out in a batch reactor, and solutions were treated with light in a quartz reaction vessel. A UV lamp (Spectroline ENF-260, 2x8W) producing 365 nm near visible light was used for photocatalytic treatments.

2.3. Synthesis and characterization of MPcs

Series of routes were followed for the synthesis of starting materials and target azomethine-bridged phenolic MPc. Fig. 1 shows the main reactions used for the synthesis. After the preparation of the (E)-4-(4-(dimethylamino)benzilideneamino) phenol and (E)-4-(4-(diethylamino)benzi-

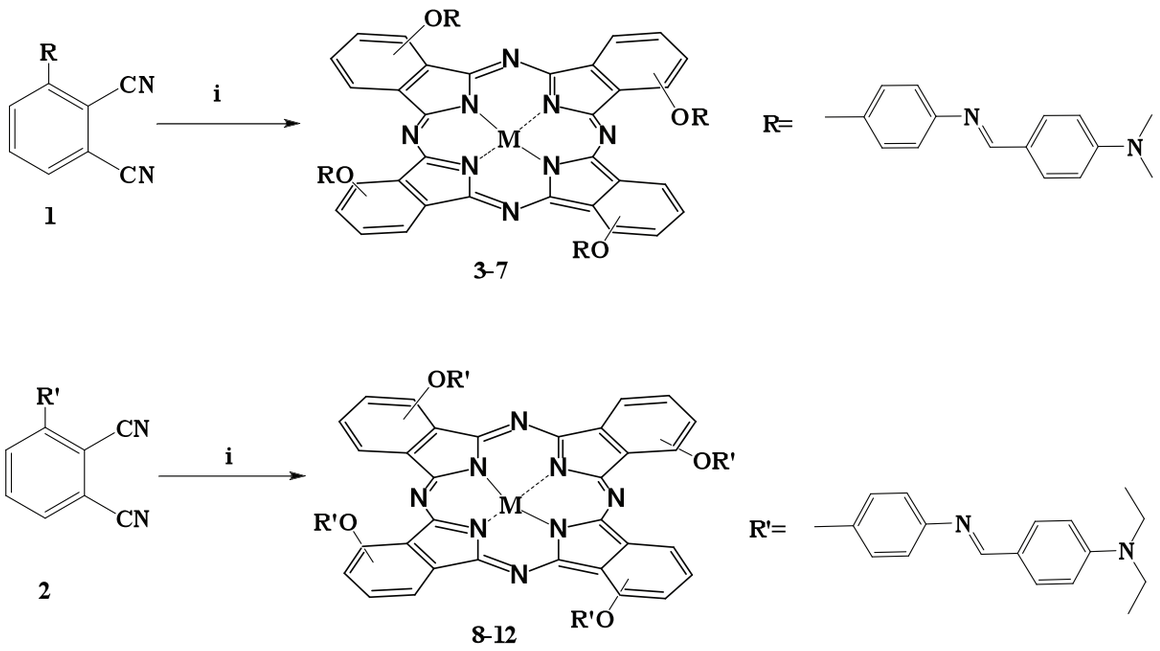

	3, 8	4, 9	5, 10	6, 11	7, 12
M	TiO	Fe	Co	Ni	Zn

i: n-pentanol, DBU for 4-7 and 9-12
n-hexanol, DBU for 3 and 8

Fig. 1. Synthetic route used for the production of MPc derivatives.

lidenamino) phenol according to literature [24], substituted phthalonitriles (1, 2) were prepared, and experimental details of these starter molecules were given in our previous study [İ. Değirmencioğlu, unpublished data]. Using these tetra-substituted phthalonitriles, 10 nonperipherally substituted MPcs (3–12) have been synthesized.

General procedure used for the synthesis is as following: 1 mmol of the substituted phthalonitriles (1, 2) and equivalent amounts of corresponding anhydrous metal salts (0.25 mmol of $Fe(Cl)_2$, $Co(Cl)_2$, $Ni(Cl)_2$ and $Zn(CH_3COO)_2$) were dissolved in sealed glass tubes in 4 mL of n-pentanol. After the addition of three drops of DBU to each solution, the temperatures were increased to 160°C. Differently from these complexes, n-hexanol and 0.50 mmol Ti(*t*-$BuO)_4$ were used for the synthesis of TiOPcs (3, 8). After the completion of the reactions, purifications were performed by column chromatography using silica gel as stationary phase. The chemical and physical characteristics of these MPcs (3–12) are given below:

Nonperipheral methylated TiOPc (3), reaction time: 10 h. Solvent system for column chromatography: Chloroform: Methanol (100:1). Yield: 0.093 g, (24.35%). IR ν_{max}/cm^{-1}: 3,035 (Ar-H), 2,969–2,926 (Alif. C-H), 1,588, 1,475, 1,329, 1,237, 1,115, 1,066, 891, 872. ^{1}HNMR ($CDCl_3$), (δ:ppm): 8.21 (s, 4H, HC=N), 7.66-7.62 (m, 20H, ArH), 7.25-7.15 (m, 8H, ArH), 6.74-6.72 (m, 16H, ArH), 3.03 (s, 24H, CH_3). UV-Vis (Chloroform): λ_{max}/nm (log ε): 723 (5.22), 695 (4.48), 659 (4.42), 377 (4.79). MS; m/z: 1,529.48 $[M+H]^+$.

Nonperipheral methylated FePc (4), reaction time: 8 h. Solvent system for column chromatography: Chloroform:Methanol (100:18). Yield: 0.102 g, (26.84%). IR ν_{max}/cm^{-1}: 3,042 (Ar-H), 2,953–2,849 (Alif. C-H), 1,583, 1,497, 1,324, 1,227, 1,172, 1,051, 953, 815. ^{1}HNMR (DMSO-d_6), (δ:ppm): 8.38 (s, 4H, HC=N), 7.64-7.51 (m, 20H, ArH), 7.33-7.18 (m, 8H, ArH), 6.78-6.70 (m, 16H, ArH), 3.11 (s, 24H, CH_3). UV-Vis (Chloroform): λ_{max}/nm (log ε): 699 (5.04), 635 (4.46), 370 (5.03). MS; m/z: 1,521.33 $[M+H]^+$.

Nonperipheral methylated CoPc (5), reaction time: 24 h. Solvent system for column chromatography: Chloroform:Methanol (100:11). Yield: 0.124 g, (32.55%). IR ν_{max}/cm^{-1}: 3,028 (Ar-H), 2,969–2,931 (Alif. C-H), 1,588, 1,478, 1,333, 1,231, 1,168, 1,088, 973, 814. UV-Vis (Chloroform): λ_{max}/nm (log ε): 695 (5.05), 634 (4.41), 351 (5.08). MS; m/z: 1,524.94 $[M+H]^+$.

Nonperipheral methylated NiPc (6), reaction time: 24 h. Solvent system for column chromatography: Chloroform:Methanol (100:5). Yield: 0.134 g, (35.20%). IR ν_{max}/cm^{-1}: 3,039 (Ar-H), 2,919–2,852 (Alif. C-H), 1,599, 1,467, 1,334, 1,226, 1,163, 1,057, 944, 813. ^{1}HNMR (DMSO-d_6), (δ:ppm): 8.23 (s, 4H, HC=N), 7.65-7.62 (m, 20H, ArH), 7.14-7.00 (bs, 8H, ArH), 6.74-6.72 (m, 16H, ArH), 3.03 (s, 24H, CH_3). UV-Vis (Chloroform): λ_{max}/nm (log ε): 695 (5.24), 624 (4.57), 347 (5.14). MS; m/z: 1,523.94 $[M+H]^+$.

Nonperipheral methylated ZnPc (7), reaction time: 24 h. Solvent system for column chromatography: Chloroform: Methanol (100:5). Yield: 0.145 g, (38.00%). IR v_{max}/cm^{-1}: 3,030 (Ar-H), 2,969–2,850 (Alif. C-H), 1,588, 1,478, 1,334, 1,240, 1,153, 1,080, 971, 818. ^{1}HNMR (DMSO-d_6), (δ:ppm): 8.35 (bs, 4H, HC=N), 7.67-7.64 (m, 10H, ArH), 7.45-7.14 (bs, 18H, ArH), 6.77-6.61 (m, 16H, ArH), 3.02 (s, 24H, CH_3) UV-Vis (Chloroform): λ_{max}/nm (log ε): 701 (5.22), 632 (4.45), 357 (4.92) MS; m/z: 1,529.84 $[M+H]^+$.

Nonperipheral ethylated TiOPc (8), reaction time: 12 h. Solvent system for column chromatography: Chloroform: Methanol (100:1). Yield: 0.096 g, (23.39%). IR v_{max}/cm^{-1}: 3,031 (Ar-H), 2,968–2,928 (Alif. C-H), 1,588, 1,478, 1,334, 1,239, 1,172, 1,079, 971, 813. ^{1}HNMR ($CDCl_3$), (δ:ppm): 8.92 (bs, 4H, HC=N), 7.68-7.24 (m, 28H, ArH), 6.38 (bs, 16H, ArH), 3.43-3.12 (bs, 16H, CH_2), 1.08-0.96 (bs, 24H, CH_3). UV-Vis (Chloroform): λ_{max}/nm (log ε): 714 (5.07), 691 (4.29), 653 (4.19), 374 (4.61). MS; m/z: 1,641.84 $[M+H]^+$.

Nonperipheral ethylated FePc (9), reaction time: 12 h. Solvent system for column chromatography: Chloroform:Methanol (100:19). Yield: 0.124 g, (30.36%). IR v_{max}/cm^{-1}: 3,045 (Ar-H), 2,956–2,849 (Alif. C-H), 1,580, 1,497, 1,325, 1,227, 1,173, 1,095, 954, 814. ^{1}HNMR (DMSO-d_6), (δ:ppm): 8.42 (s, 4H, HC=N), 7.69-7.55 (m, 10H, ArH), 7.56-7.35 (bm, 6H, ArH), 7.29-7.20 (m, 6H, ArH), 7.09-6.98 (m, 6H, ArH), 6.72-6.55 (m, 16H, ArH), 3.42-3.36 (q, 16H, CH_2), 1.15-1.09 (t, 24H, CH_3). UV-Vis (Chloroform): λ_{max}/nm (log ε): 696 (4.95), 633 (4.44), 371 (4.12). MS; m/z: 1,633.39 $[M+H]^+$.

Nonperipheral ethylated CoPc (10), reaction time: 24 h. Solvent system for column chromatography: Chloroform:Methanol (100:11). Yield: 0.139 g, (33.97%). IR v_{max}/cm^{-1}: 3,035 (Ar-H), 2,966–2,927 (Alif. C-H), 1,591, 1,474, 1,330, 1,240, 1,173, 1,080, 979, 813. UV-Vis (Chloroform): λ_{max}/nm (log ε): 698 (5.07), 635 (4.40), 353 (5.24). MS; m/z: 1,183.46 $[M-C_{30}H_{36}N_4]^+$.

Nonperipheral ethylated NiPc (11), reaction time: 24 h. Solvent system for column chromatography: Chloroform:Methanol (100:4). Yield: 0.149 g, (36.42%). IR v_{max}/cm^{-1}: 3,047 (Ar-H), 2,923–2,849 (Alif. C-H), 1,599, 1,504, 1,351, 1,227, 1,173, 1,058, 957, 817. ^{1}HNMR (DMSO-d_6), (δ:ppm): 8.24 (s, 4H, HC=N), 7.61-7.56 (m, 8H, ArH), 7.21-7.03 (bs, 16H, ArH), 6.71-6.62 (m, 20H, ArH), 3.43-3.37 (q, 16H, CH_2), 1.12-0.94 (t, 24H, CH_3). UV-Vis (Chloroform): λ_{max}/nm (log ε): 699 (4.79), 639 (4.21), 371 (4.62). MS; m/z: 1,637.81 $[M+3]^+$.

Nonperipheral ethylated ZnPc (12), reaction time: 24 h. Solvent system for column chromatography: Chloroform:Methanol (100:3). Yield: 0.187 g, (45.52%). IR v_{max}/cm^{-1}: 3,033 (Ar-H), 2,933–2,851 (Alif. C-H), 1,589, 1,478, 1,332, 1,237, 1,166, 1,089, 971, 815. ^{1}HNMR (DMSO-d_6), (δ:ppm): 8.36 (s, 4H, HC=N), 7.71-7.62 (m, 10H, ArH), 7.53-7.44 (m, 6H, ArH), 7.30-7.22 (m, 6H, ArH), 7.13-7.03 (m, 6H, ArH), 6.75-6.61 (m, 16H, ArH), 3.44-3.41 (q, 16H, CH_2), 1.12-1.08 (t, 24H, CH_3). UV-Vis (Chloroform): λ_{max}/nm (log ε): 706 (5.29), 641 (4.52), 361 (4.62). MS; m/z: 1,641.84 $[M+H]^+$.

2.4. Preparation of MPc/TiO_2 composites

MPcs were nonperipheral substituted form, and MPc/TiO_2 nanocomposites were prepared by following the procedure reported by Sun et al. [25]. Firstly, a certain weight of each MPc was dispersed in 1 mL dimethly formamide (DMF), and this solution was slowly added to the TiO_2 suspension (2 g/L). The mass of MPc was 1% of TiO_2 mass. The mixture was stirred for 24 h at ambient temperature for anchoring of MPc molecules. Finally, precipitates were filtered through a membrane (pore diameter, 0.45 μm), washed several times with distilled water and dried in vacuum at 80°C for 6 h. The amount of the adsorbed MPc on TiO_2 was determined by measuring the remaining concentration of MPc in reaction mixture before and after adsorption.

2.5. Photocatalytic experiments

The experiments for Cr(VI) photoreduction were carried out in a quartz cell equipped with a 365 nm UV lamp (6 W, Type ENF-260C, Spectroline, at a light intensity of 350 mW/cm_2). The distance between the light source and the reaction cell was 10 cm. For typical experiments, suspensions was prepared by adding 40 mg of the composite powder into a 20 mL $K_2Cr_2O_7$ aqueous solution (10 mg/L Cr(VI)) at pH 2. The pH of the working solutions was adjusted with H_3PO_4. The reaction mixture was maintained in suspension by using a magnetic stirrer in the absence and presence of the light. At the appropriate time intervals, 2 mL portions were sampled and immediately centrifuged at 4,000 rpm for 20 min to remove any suspended solid photocatalyst particles. The supernatant was separated and analyzed for residual Cr(VI) ions. Standard diphenylcarbazide colorimetric method was used for measurement [22]. The percentage of photocatalytic reduction was calculated using the equation given below:

$$\text{Photocatalytic reduction (\%)} = \frac{[C]_0 - [C]_t}{[C]_0} \times 100 \quad (1)$$

in which C_0 is the initial Cr(VI) concentration, and C is the residual Cr(VI) concentration after treatment. The results are given as mean of three replicates.

3. Results and discussion

3.1. Synthesis and characterization of MPcs (3–12)

The synthetic pathway used during the preparation of the MPcs was already given in Fig. 1. The characterizations of the structures of new compounds have been performed by a combination of ^{1}H and ^{13}C-NMR, FT-IR, UV-Vis spectroscopy and mass spectral data.

The preparations of the new 1(4),8(11),15(18),22(25)-tetra-substituted (nonperipheral positions) MPc complexes (3–12) were performed by cyclotetramerization of the tetra-substituted phthalonitriles (1, 2) with corresponding metal salts. The products of the cyclotetramerization reactions were in an isomeric mixture, as expected. These four possible isomers are C_{4h}, C_{2v}, C_s and D_{2h}, and the composition of them depends on central metal ion and the shape

of the substituents for nonperipherally tetra-substituted phthalocyanines [26]. There was no need to separate this mixture, and therefore, no attempt was made to separate them. The purifications of the MPcs (3–12) were performed by column chromatograph with silica gel. The solubility of all phthalocyanine dyes are good in organic solvents such as chloroform, dichloromethane, tetrahydrofuran, DMSO and DMF.

In the Infrared Spectroscopy (IR) spectra of MPcs (3–12), the most important evidences of the occurrence of the cyclotetramerizations of the substituted phthalonitriles (1, 2) to MPcs were the disappearances of the C≡N vibrations at 2,230 cm^{-1} [İ. Değirmencioğlu, unpublished data]. ^{1}H-NMR measurement of CoPcs (5 and 10) could not be performed because of the presence of the paramagnetic cobalt(II) ion in the cavity of the phthalocyanine rings [27]. The ^{1}H-NMR spectra of the other complexes were very similar to that of their corresponding starting compounds (1, 2). In the mass spectra of the substituted MPcs (3–12), parent molecular ion peaks at m/z = 1,529.48 $[M+H]^+$, 1,521.33 $[M+H]^+$, 1,524.94 $[M+H]^+$, 1,523.94 $[M+H]^+$, 1,528.91 $[M+H]^+$, 1,529.84 $[M+H]^+$, 1,641.84 $[M+H]^+$, 1,633.39 $[M+H]^+$, 1,183.46 $[M–C_{30}H_{36}N_4]^+$, 1,637.81 $[M+3]^+$, 1,640.88 $[M+H]^+$ and 1,641.84 $[M+H]^+$, respectively, verified the proposed structures.

"B" or "Soret" bands (at 300–500 nm) and Q-bands (at 600–750 nm) are the absorption regions of phthalocyanines in their ground state electronic spectra. Due to their degenerate D_{4h} symmetry, the Q-bands of MPcs are generally observed as single strong absorption band. Furthermore, their aggregation behavior, association of the molecules in solution, can be determined from their electronic spectra [28]. The absorption spectra of MPcs (3–12) in chloroform at 1 × 10^{-5} M concentration are shown in Figs. 2 and 3.

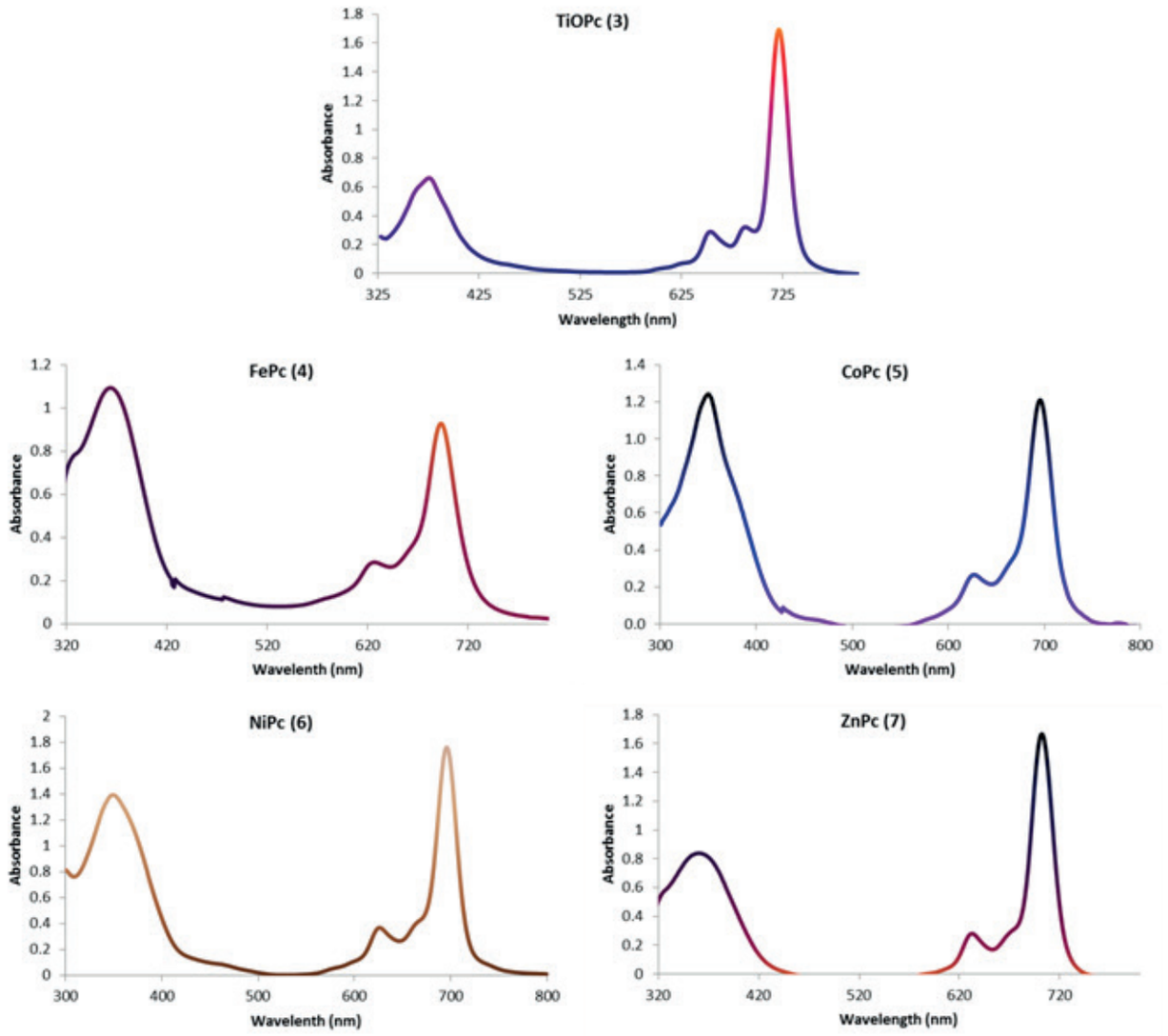

Fig. 2. UV-Vis spectra of compounds 3–7 in chloroform at 1 × 10^{-5} M concentration.

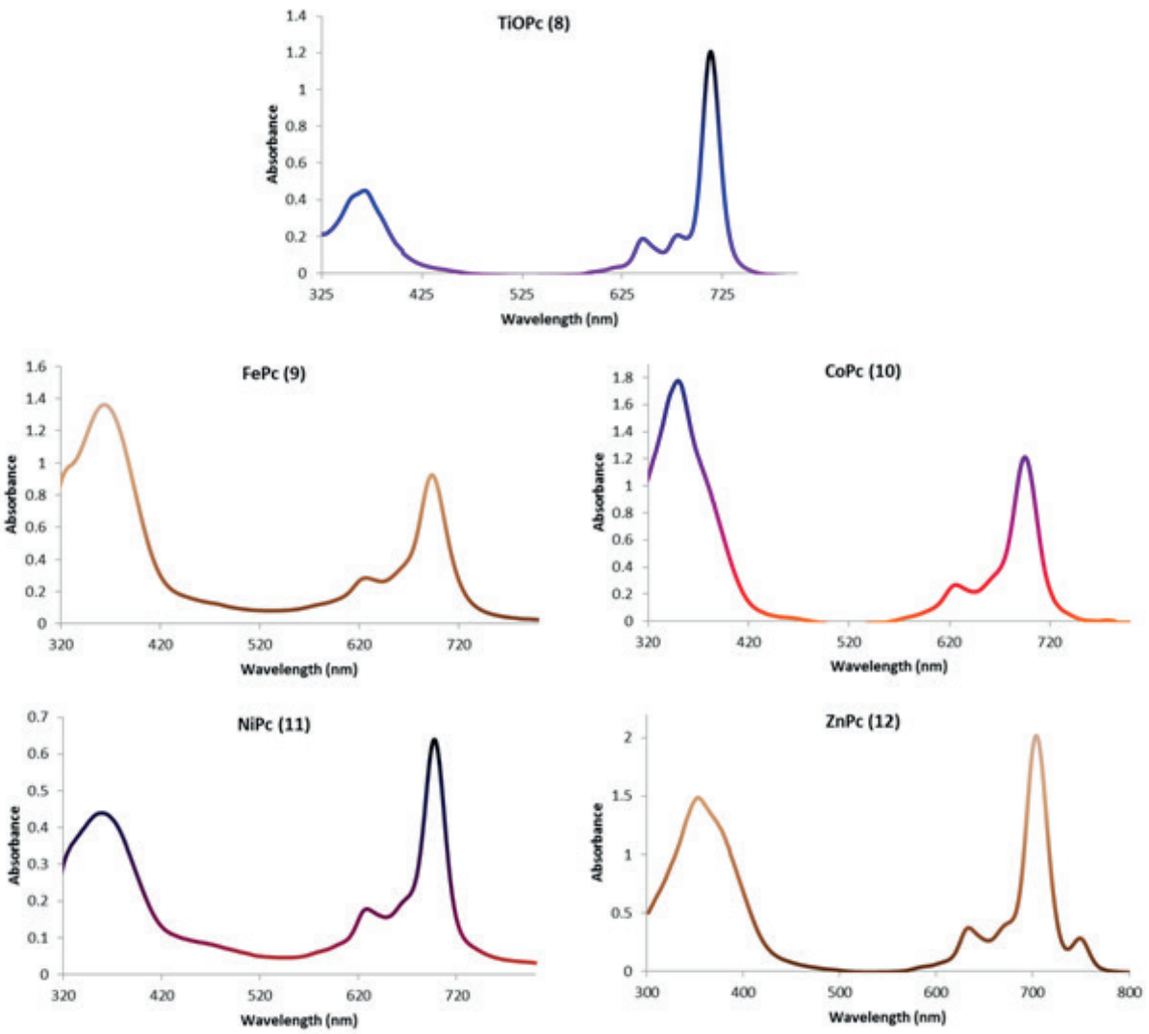

Fig. 3. UV-Vis spectra of compounds 8–12 in chloroform at 1×10^{-5} M concentration.

Strong single Q-bands, evidence of the degenerate D_{4h} symmetry, were observed at 723 nm for TiOPc (3), 699 nm for FePc (4), 695 nm for CoPc (5), 695 nm for NiPc (6), 701 nm for ZnPc (7), 714 nm for TiOPc (8), 696 nm for FePc (9), 698 nm for CoPc (10), 699 nm for NiPc (11), and 706 nm for ZnPc (12). As can be seen from the figures, sharp Q-bands are the evidence of their monomeric behavior in chloroform at 1×10^{-5} M concentration. Finally the B-bands of all MPcs were observed at around 355–380 nm.

3.2. Evaluation of photocatalytic activity of photocatalysts

The amount of MPc immobilized on TiO_2 was determined from its residual concentration in aqueous medium. MPc derivatives exhibited good attachment on TiO_2 surface, and immobilized percentages are given in Table 1.

The MPc derivatives were easily adsorbed onto TiO_2 from DMF solution. Stability of the immobilization was checked with desorption studies. MPc/TiO_2 powder was suspended in water and stirred for 24 h, and concentration of released MPc was monitored at certain intervals. None of the composites released absorbed MPc molecule indicating that MPc derivatives are strongly attached on TiO_2. The photocatalytic activities of MPc/TiO_2 nanocomposites were measured for removal of aqueous Cr(VI) solution (10 mg/L) during 150 min irradiation with a near visible light (365 nm). Fig. 4 shows the removal percentage of Cr(VI) ions employing prepared catalysts for 150 min exposure period. Triplicate runs were carried out for each test, and the relative standard deviation was generally less than 1%.

The photocatalytic reduction of Cr(VI) is clearly more effective with MPc/TiO_2 composite materials than bare TiO_2. The substituted R group on Pc macrocycle containing methyl groups seems to me more effective for TiOPc/TiO_2, FePc/TiO_2 and NiPc/TiO_2, than ethylated ones. CoPc/TiO_2 and ZnPc/TiO_2 exposed relatively higher reduction ability among ethylated ones.

Table 1
Immobilization percentages of MPcs on TiO_2 surface

Comp. No.	$TiOPc/TiO_2$		$FePc/TiO_2$		$CoPc/TiO_2$		$NiPc/TiO_2$		$ZnPc/TiO_2$	
	Methyl	Ethyl	Methyl	Ethyl	Methyl	Ethyl	Methyl	Ethyl	Methyl	Ethyl
	(3)	(8)	(4)	(9)	(5)	(10)	(6)	(11)	(7)	(12)
% (w/w)	0.92	0.95	0.95	0.96	0.95	0.93	0.92	0.95	0.90	0.96

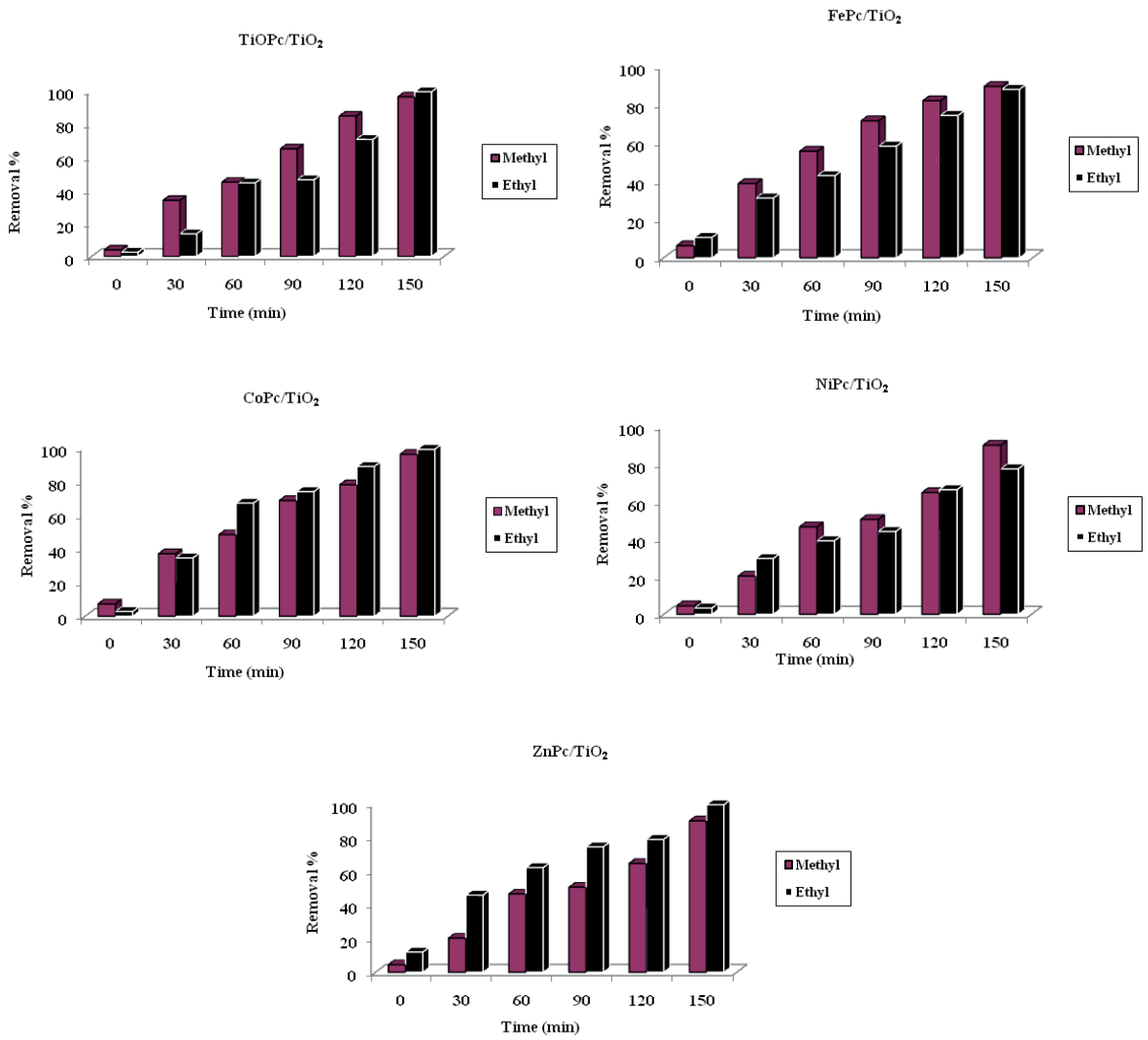

Fig. 4. The removal percentage of Cr(VI) ions with MPc/TiO_2 (methylated and ethylated) catalysts using 365 nm light.

The Cr(VI) reduction percentage of the each catalyst was compared in Fig. 5 after a 150 min of irradiation. For a better understanding, Cr(VI) removal percentage of metal-free Pc and bare TiO_2 were also included in Fig. 5 to evaluate the contribution of metal for electron transfer. Metal-free Pc (defined as H_2Pc/TiO_2) has the same macrocyclic molecule containing azomethine-bridged phenolic substitution at nonperipheral position (methylated and ethylated) except the metal ion in the center. Details of the photocatalytic action of H_2PcTiO_2 composite has been discussed elsewhere [İ. Değirmencioğlu, unpublished data]. Figure also show the removal rate of Cr(VI) ions in the absence of light (given as black columns). It is clear that the light is the main component of the photoreduction.

In MPc derivatives containing methyl groups provided the removal rates between 88.68% and 99.27% in the following order: $CoPc/TiO_2$ (99.3%) > $TiOPc/TiO_2$ (96.6%) > $ZnPc/TiO_2$ (94.3%) > H_2Pc/TiO_2 (92.4%) > $NiPc/TiO_2$ (89.7%) > $FePc/TiO_2$ (89.6%) > TiO_2 (55.4%). On the other hand ethyl

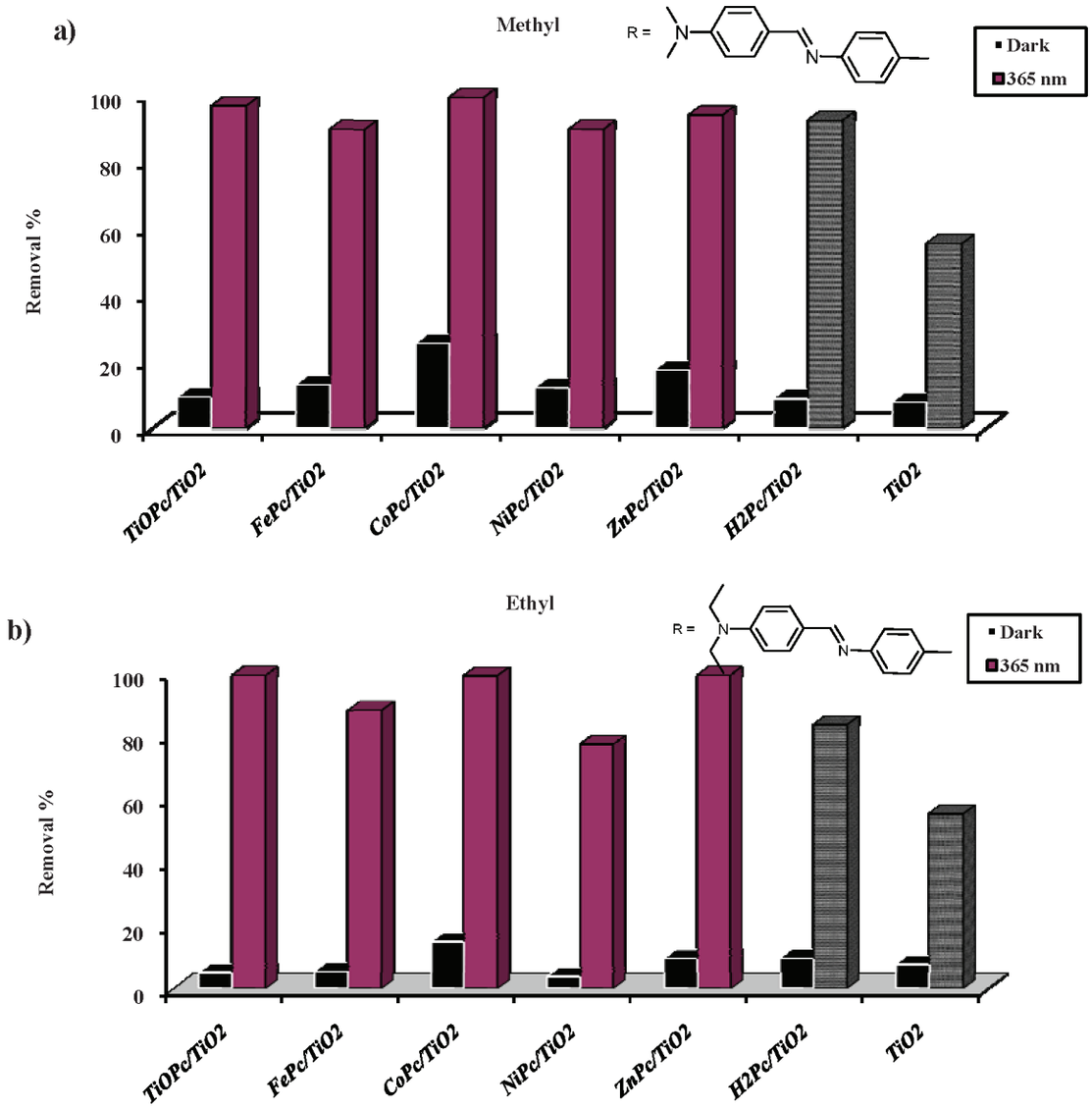

Fig. 5. The removal percentages of Cr(VI) ions with MPc/TiO_2 catalysts containing: (a) methyl and (b) ethyl groups, metal-free Pc and bare TiO_2 after 150 min exposure (λ = 365 nm).

containing derivatives showed different tendency in the following order: TiOPc/TiO_2 (99.5%) = ZnPc/TiO_2 (99.5%) > CoPc/TiO_2 (99.0%) > FePc/TiO_2 (88.1%) > H_2Pc/TiO_2 (83.7%) > NiPc/TiO_2 (77.4%) > TiO_2 (55.4%). The experimental results demonstrated that the presence of MPc plays a significant role in enhancing TiO_2 photocatalytic activity under near UV-Vis light irradiation. Sensitization of TiO_2 with Pc greatly enhances the electron transfer. Electrons generated by excited MPc are transferred into the conduction band (CB) of TiO_2, leading to effective reduction of Cr(VI) ions by excess electrons. Thus, the photo-reduction efficiency of Cr(VI) is greatly enhanced due to facilitated electron transfer. Possible electron transfer pathway is illustrated in Fig. 6. In particular, CoPc, TiOPc and ZnPc sensitized TiO_2 has higher photocatalytic reduction ability compared with other catalysts.

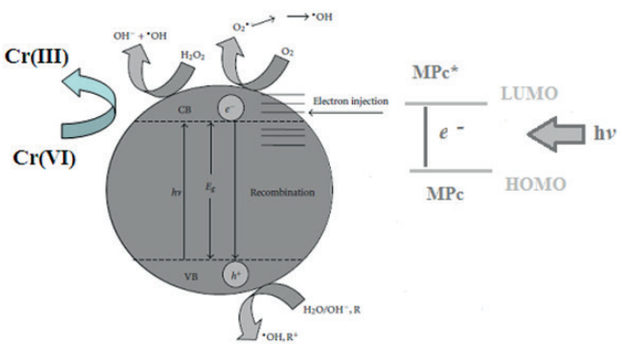

Fig. 6. Possible electron transfer pathway.

Electron transfer ability of studied MPc molecules can be evaluated according to central metal ion and methylated/ethylated substitution. These are given below:

- First of all, both methylated and ethylated substituents have electron donor groups. This prevents the possibility of aggregation as well as obstruction of inner charge transfer in the molecule. As a result of this effect electron transfer from MPc to TiO_2 is eased.
- MPc derivatives have planar geometry that fosters the effective electron transfer. Additionally, orientation of methylated/ethylated substituent (vertical or angular) at peripheral position also affects the electron transfer from MPc to TiO_2.
- All MPc derivatives might have a higher LUMO energy level than conductive band of neat TiO_2. Due to good electronic coupling electron transfer is high leading to effective reduction of Cr(VI).
- Enhanced photo-reduction can be explained with obstruction of *inner-path* and *outer-path* electron transfer of MPc molecule that is attached on TiO_2 surface. This obstruction channels the electron of MPc to TiO_2 and Cr(VI) ions in near environment (Fig. 6).
- Azomethine-bridged phenolic groups (methylated and ethylated derivatives, substituted at nonperipheral position) are relatively nonpolar compared with electrolyte solvent. This might prevent approaching the electrolyte onto TiO_2 but provoke electron transfer from MPc/TiO_2 to Cr(VI) ions.
- Chemically, MPc molecule tends to preserve its stability via employing photogenerated electrons in photocurrent cycle. This action also provokes the reduction of Cr(VI) ions.
- Both methylated and ethylated derivatives of CoPc seem to be highly effective for electron transfer. This might be due to paramagnetic nature of Co(II) ion in the center and indicated the importance of metal ion in macrocylic ring.

Not only one factor is dominant but also all these factors might affect the photocatalytic reduction of Cr(VI) ions. It is not easy to explain "why different metal ion incorporated phtalocyanine molecule has different photocatalytic action?" For example, CoPc/TiO_2 has the highest activity while FePc/TiO_2 has the lowest activity among methylated derivatives. However, TiOPc/TiO_2 has the highest activity while NiPc/TiO_2 has the lowest activity among ethylated derivatives [29].

3.3. Computational details

These all calculations were performed with the GaussView 5 molecular visualization program and Gaussian 09 program package [30,31]. The quantum chemical computations of all compounds were performed by using Becke's three parameter exact exchange-functional (B3) combined with gradient-corrected correlational functional of Lee, Yang, Parr (LYP) [32,33] with the 6-31G(d) basis set that was Pople double-zeta basis set with polarizing d-functions on heavy atoms. All computations were carried out in the ground state in the gas phase of the compounds and the 6-31G(d) basis set was used for all atoms.

3.4. The highest occupied molecular orbital (HOMO) and LUMO analyses

In order to gain an insight into the molecular structure and electron distribution, density functional theory calculations were performed on ten substituted Mcs using the Gaussian 03/09 program packages. As also shown in Fig. 7, due to the nature of the phthalocyanine molecule, the central cavity of the molecule is planar. The complexes that have groups on their nonperipheral positions have less planarity. Such a coplanar conformation is a desirable condition since it allows sizable orbital overlap between the donor and intervening azomethine linker. Therefore, the change in electron distribution caused by photoexcitation may lead to an efficient charge separation. It is clearly seen that the HOMO-LUMO excitation by light irradiation could move electron distribution to the side of the methylated/ethylated nitrogen from the isoindoline unit, and therefore, the photoinduced electron transfer from the dye to the TiO_2 electrode can occur efficiently by the HOMO-LUMO transition. Due to their broader ΔE energy gaps, red shifting of the spectrum and π/π^* distribution with higher character in LUMOs of CoPc, TiOPc and ZnPc dyes, the nitrogen atoms at nonperipheral position should enhance the orbital overlapping with 3d orbital of the titanium and subsequently favor the electron injection to the conduction band of TiO_2 and thus, the Cr(VI) ion is reduced to Cr(III) ion easily. The breaking of the conjugation produced by the methylene in the ethylated species, Cr(VI) ion, is caused to the reduction with lower data. Also, having higher LUMO energy of all MPcs than the TiO_2 conduction band and lower HOMO energy levels than the redox potential of the solution are additional contributions for efficient regeneration of the dye cation [34–37].

The HOMO, LUMO and HOMO-LUMO energy values for all compounds were listed in Table 2. Similarly, the HOMO and LUMO shapes for all compounds were given in Fig. 7. In all compounds, the HOMOs are almost localized over phthalocyanine groups, while the LUMOs are almost localized over phthalocyanine ones and central metal atoms. But, the LUMO in the compound 4 is only localized over central Fe atom.

4. Conclusions

In this work, we have successfully prepared a series of novel nonperipheral substituted phthalocyanines (MPcs) and used these derivatives for sensitization of TiO_2. Experimental results revealed that the photocatalytic reduction capability of TiO_2 under near visible light irradiation has been greatly increased with incorporation of MPc. These MPc/TiO_2 nanocomposites might be good candidates for application of dye-sensitized solar cells (DSSC) as well as phocatalytic applications. The concentration of immobilized MPc is extremely low but enough for effective absorption of photons from light. Theoretical calculations show that the delocalization of the excited state is broken between azomethine linker and ethylated nitrogen atoms, which is unfavorable for electron injection from related dyes 8–12 to the conduction band of the TiO_2. Further structural optimizations, such as broadening absorption spectra and tuning energy levels, are very promising to generate more efficient sensitizers.

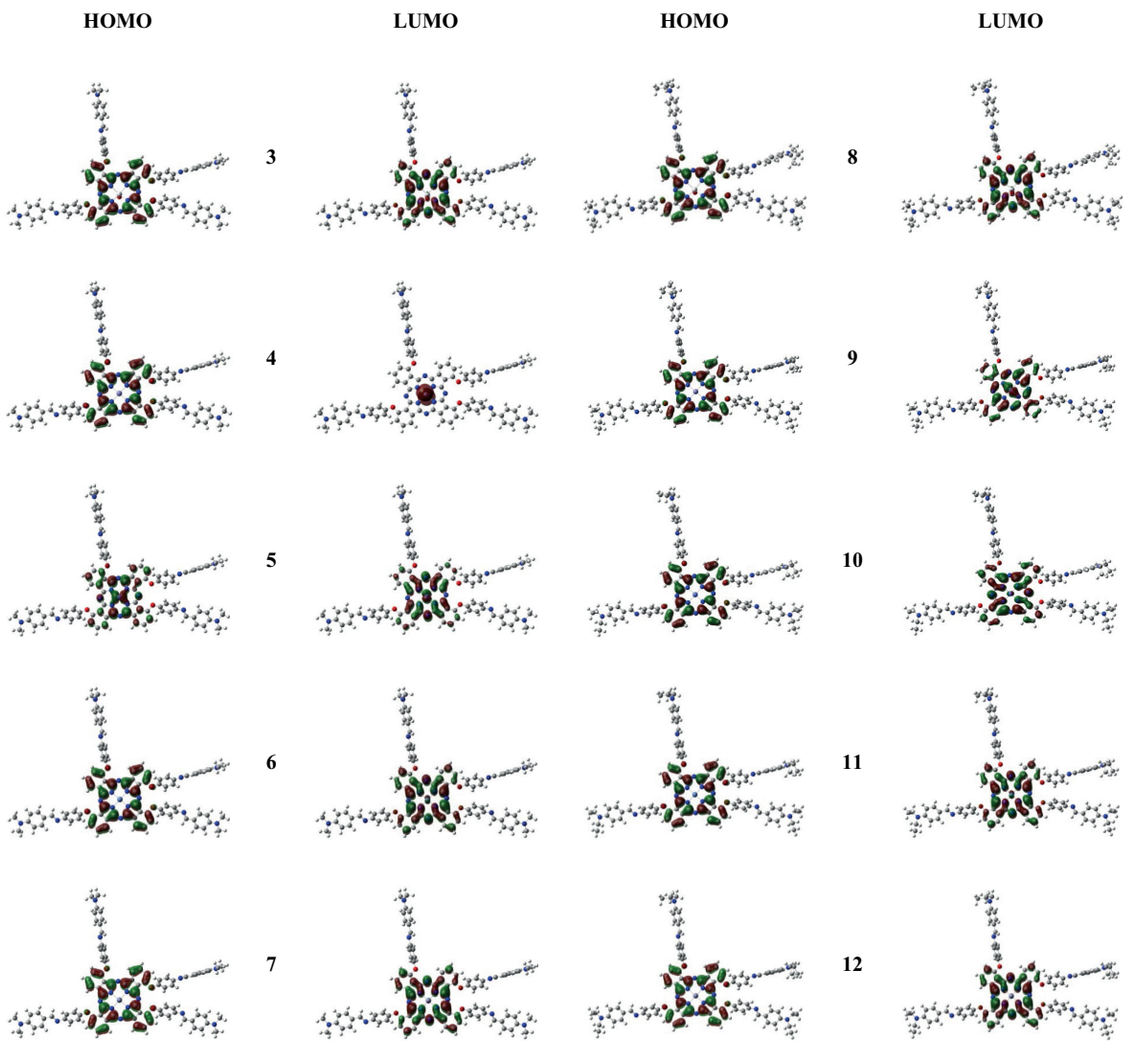

Fig. 7. The HOMO and LUMO shapes for all compounds.

Table 2
The HOMO, LUMO and HOMO-LUMO energy values of all compounds

Compound	E(HOMO) (eV)	E(LUMO) (eV)	|E(HOMO)-E(LUMO)| (eV)
3	–4.49722	–2.48685	2.01038
4	–4.35001	–2.73229	1.61772
5	–3.85776	–1.73391	2.12385
6	–4.36661	–2.24603	2.12058
7	–4.36933	–2.30208	2.06725
8	–4.47654	–2.46263	2.01391
9	–4.35219	–2.84087	1.51132
10	–4.36470	–2.57664	1.78806
11	–4.35545	–2.23460	2.12085
12	–4.35654	–2.28848	2.06806

Acknowledgement

The authors gratefully appreciate the financial support from Turkish Scientific Research Council (TUBITAK, Project No.: 113Z308). The authors declare that there is no conflict of interest.

References

[1] B.H. Vilsinski, A.P. Gerola, J.A. Enumo, K.D.S. Campanholi, P.C.D. Pereira, G. Braga, N. Hioka, E. Kimura, A.L. Tessaro, W. Caetano, Formulation of aluminum chloride phthalocyanine in Pluronic™ P-123 and F-127 block copolymer micelles: photophysical properties and photodynamic inactivation of microorganisms, Photochem. Photobiol. 91 (2015) 518–525.
[2] N. Nombona, P. Tau, N. Sehlotho, T. Nyokong, Electrochemical and electrocatalytic properties of α-substituted manganese and titanium phthalocyanines, Electrochim. Acta, 53 (2008) 3139–3148.
[3] M. Camerin, M. Magaraggia, M. Soncin, G. Jori, M. Moreno, I. Chambrier, The *in vivo* efficacy of phthalocyanine-nanoparticle

conjugates for the photodynamic therapy of amelanotic melanoma, Eur. J. Cancer, 46 (2010) 1910–1918.
[4] A. Moussaron, P. Arnoux, R. Vanderesse, E. Sibille, P. Chaimbault, C. Frochot, Lipophilic phthalocyanines for their potential interest in photodynamic therapy: synthesis and photo-physical properties, Tetrahedron, 69 (2013) 10116–10122.
[5] V. Parra, M. Bouvet, J. Brunet, M.L. Rodriguez-Mendez, J.A. Saja, On the effect of ammonia and wet atmospheres on the conducting properties of different lutetium bisphthalocyanine thin films, Thin Solid Films, 516 (2008) 9012–9019.
[6] M. Bouvet, Phthalocyanine-based field-effect transistors as gas sensors, Anal. Bioanal. Chem., 384 (2006) 366–373.
[7] F. Yang, S.R. Forrest, Photocurrent generation in nanostructured organic solar cells, ACS Nano, 2 (2008) 1022–1032.
[8] M. Selçukoğlu, E. Hamuryudan, Novel phthalocyanines with pentafluorobenzyloxy-substituents, Dyes Pigm., 74 (2007) 17–20.
[9] S. Sürgün, Y. Arslanoğlu, E. Hamuryudan, Synthesis of non-peripherally and peripherally substituted zinc (II) phthalocyanines bearing pyrene groups via different routes and their photophysical properties, Dyes Pigm., 100 (2014) 32–40.
[10] İ. Altın, M. Sökmen, Photocatalytic properties of silver incorporated titania nanoparticles immobilized on waste-derived polystyrene, Water Air Soil Pollut., 225 (2014) 1786–1788.
[11] L. Kuai, B.Y. Geng, X.T. Chen, Y.Y. Zhao, Y.C. Luo, Facile subsequently light-induced route to highly efficient and stable sunlight-driven Ag-AgBr plasmonic photocatalyst, Langmuir, 26 (2010) 18723–18727.
[12] S.T. Finn, J.A. Strnad, P.D. Barreto, M.E. Fox, J. Torres, J.D. Sweeney, J.C. Barreto, A screening technique useful for testing the effectiveness of novel "self-cleaning" photocatalytic surfaces, Photochem. Photobiol., 87 (2011) 1184–1188.
[13] İ. Tatlıdil, E. Bacaksız, C.K. Buruk, C. Breen, M. Sökmen, A short literature survey on iron and cobalt ion doped TiO_2 thin films and photocatalytic activity of these films against fungi, J. Alloys Compd., 517 (2012) 80–86.
[14] W. Baran, A. Makowske, W. Wardas, The effect of UV radiation absorption of cationic and anionic dye solutions on their photocatalytic degradation in the presence TiO_2, Dyes Pigm., 76 (2008) 226–230.
[15] N. Yazdanpour, S. Sharifnia, Photocatalytic conversion of green house gases (CO_2 and CH_4) using copper phthalocyanine modified TiO_2, Sol. Energy Mater. Sol. Cells, 118 (2013) 1–8.
[16] L. Li, X. Bai-fu, Photogenerated carrier transfer mechanism and photocatalysis properties of TiO_2 sensitized by Zn(II) phthalocyanine, J. Cent. South Univ. T., 17 (2010) 218–222.
[17] E. Evgenidou, K. Fytianos, I. Poulios, Semiconductor sensitized photodegradation of dichlorvos in water using TiO_2 and ZnO as catalysts, Appl. Catal., B, 59 (2005) 81–89.
[18] V. Iliev, D. Tomova, Photocatalytic oxidation of sulfide ion catalyzed by phthalocyanine modified titania, Catal. Commun., 3 (2002) 287–292.
[19] E. Vargas, R. Vargas, A. Oswaldo Nunez, TiO_2 surface modified with copper(II) phthalocyanine-tetrasulfonic acid tetrasodium salt as a catalyst during photoinduced dichlorvos mineralization by visible solar light, Appl. Catal., B, 156–157 (2014) 8–14.
[20] Z. Huang, B. Zheng, S. Zhu, Y. Yao, Y. Ye, W. Lu, W. Chen, Photocatalytic activity of phthalocyanine-sensitized TiO_2–SiO_2 microparticles irradiated by visible light, Mater. Sci. Semicond. Process., 25 (2014) 148–152.
[21] Z. Zhao, J. Fan, M. Xie, Z. Wang, Photocatalytic reduction of carbon dioxide with in-situ synthesized CoPc/TiO_2 under visible light irradiation, J. Clean. Prod., 17 (2009) 1025–1029.
[22] Ş. Akkan, İ. Altın, M. Koç, M. Sökmen, TiO_2 immobilized PCL for photocatalytic removal of hexavalent chromium from water, Desal. Wat. Treat., 56 (2015) 2522–2531.
[23] D.D. Perrin, W.L.F. Armarego, Purification of Laboratory Chemicals, Pergamon, Oxford, 1989.
[24] S.T. Ha, L.K. Ong, Y. Sivasothy, Y.F. Win, Synthesis of new schiff bases with dialkylamino end groups and effect of terminal branching on mesomorphic properties, World Appl. Sci. J., 8 (2010) 641–646.
[25] Q. Sun, Y. Xu, Sensitization of TiO_2 with aluminum phthalocyanine: factors influencing the efficiency for chlorophenol degradation in water under visible light, J. Phys. Chem. C, 113 (2009) 12387–12394.
[26] A. Erdogmuş, M. Durmuş, A.L. Uğur, O. Avcıata, U. Avcıata, T. Nyokong, Synthesis, photophysics, photochemistry and fluorescence quenching studies on highly soluble substituted oxo-titanium(IV) phthalocyanine complexes, Synth. Met., 160 (2010) 1868–1876.
[27] R. Bayrak, H.T. Akçay, M. Pişkin, M. Durmuş, İ. Değirmencioğlu, Azine-bridged binuclear metallophthalocyanines functioning photophysical and photochemical-responsive, Dyes Pigm., 95 (2012) 330–337.
[28] R. Bayrak, K. Karaoğlu, Y. Ünver, K. Sancak, F. Dumludağ, İ. Değirmencioğlu, Synthesis, characterization, spectral and electrical properties of peripherally tetratriazole-substituted phthalocyanines and its metal complexes, J. Organomet. Chem., 712 (2012) 57–66.
[29] B.G. Kim, K. Chung, J. Kim, Molecular design principle of all-organic dyes for dye-sensitized solar cells, Chem. Eur. J., 19 (2013) 5220–5230.
[30] M.J. Frisch, G.W. Trucks, H.B. Schlegel, G.E. Scuseria, M.A. Robb, J.R. Cheeseman, G. Scalmani, V. Barone, B. Mennucci, G.A. Petersson, H. Nakatsuji, M. Caricato, X. Li, H.P. Hratchian, A.F. Izmaylov, J. Bloino, G. Zheng, J.L. Sonnenberg, M. Hada, M. Ehara, K. Toyota, R. Fukuda, J. Hasegawa, M. Ishida, T. Nakajima, Y. Honda, O. Kitao, H. Nakai, T. Vreven, J.A. Montgomery Jr., J.E. Peralta, F. Ogliaro, M. Bearpark, J.J. Heyd, E. Brothers, K.N. Kudin, V.N. Staroverov, R. Kobayashi, J. Normand, K. Raghavachari, A. Rendell, J.C. Burant, S.S. Iyengar, J. Tomasi, M. Cossi, N. Rega, J.M. Millam, M. Klene, J.E. Knox, J.B. Cross, V. Bakken, C. Adamo, J. Jaramillo, R. Gomperts, R.E. Stratmann, O. Yazyev, A.J. Austin, R. Cammi, C. Pomelli, J.W. Ochterski, R.L. Martin, K. Morokuma, V.G. Zakrzewski, G.A. Voth, P. Salvador, J.J. Dannenberg, S. Dapprich, A.D. Daniels, Ö. Farkas, J.B. Foresman, J.V. Ortiz, J. Cioslowski, D.J. Fox, Gaussian 09, Revision C.01, Gaussian Inc, Wallingford, CT, 2009.
[31] R. Dennington, T. Keith, J. Millam GaussView, Version 5, Semichem Inc., Shawnee Mission, KS, 2009.
[32] A.D. Becke, Density-functional thermochemistry. III. The role of exact exchange, J. Chem. Phys., 98 (1993) 5648–5652.
[33] C. Lee, W. Yang, R.G. Parr, Development of the Colle-Salvetti correlation-energy formula into a functional of the electron density, Phys. Rev. B: Condens. Matter, 37 (1988) 785–789.
[34] N. Santhanamoorthi, K.H. Lai, F. Taufany, J.C. Jiang, Theoretical investigations of metal-free dyes for solar cells: Effects of electron donor and acceptor groups on sensitizers, J. Power Sources, 242 (2013) 464–471.
[35] P. Shen, X. Liu, S. Jiang, Y. Huang, L. Yi, B. Zhao, S. Tan, Effects of aromatic π-conjugated bridges on optical and photovoltaic properties of N,N-diphenylhydrazone-based metal-free organic dyes, Org. Electron., 12 (2011) 1992–2002.
[36] L. Yang, L. Guo, Q. Chen, H. Sun, H. Yan, Q. Zeng, X. Zhang, X.Pan, S. Dai, Substituent effects on zinc phthalocyanine derivatives: a theoretical calculation and screening of sensitizer candidates for dye-sensitized solar cells, J. Mol. Model., 38 (2012) 82–89.
[37] L. Giribabu, V.K. Singh, T. Jella, Y. Soujanya, A. Amat, F. De Angelis, A. Yella, P. Gao, M.K. Nazeeruddin, Sterically demanded unsymmetrical zinc phthalocyanines for dye-sensitized solar cells, Dyes Pigm., 98 (2013) 518–529.